

PACS numbers: 42.55.Lt; 42.60.Jf; 42.60.Lh
DOI: 10.1070/QE2009v039n10ABEH014100

Gas-discharge laser on a self-terminating thallium transition

P.A. Bokhan, Dm.E. Zakrevskii, M.A. Lavrukhin

***Abstract*. We report an experimental study of the performance parameters of a gas discharge pumped thallium vapour laser operating on the $7s\,^2S_{1/2} - 6p\,^2P^o_{3/2}$ self-terminating transition at 535 nm. The switch we used, a TPI3-10k/25 cold-cathode thyratron, ensures a rise time of the load voltage pulse less than 15 ns. The laser output power is shown to increase in proportion to the energy stored in the discharge capacitor (up to the maximum voltage of the thyratron). The optimal pump pulse repetition rate for He(Ne) – Tl mixtures is ~ 1.75 kHz. Even small hydrogen additions reduce the lasing energy and average output power. The addition of bismuth vapour increases the optimal pulse repetition rate (up to 3 kHz) and average output power. The factors responsible for the lower lasing efficiency in comparison with the copper vapour laser are analysed.**

Keywords: *thallium vapour laser, self-terminating transition, gas discharge*.

1. Introduction

Thallium vapour lasers operating on the $7s\,^2S_{1/2} - 6p\,^2P^o_{3/2}$ self-terminating transition ($\lambda = 535$ nm) are of interest for a number of applications, which is associated primarily with the use of thallium isotopes in medicine. ^{203}Tl is a raw material for ^{201}Tl-based radiopharmaceuticals intended for the early detection and management of cancerous growths of various etiologies in soft tissues and inflammatory foci, as well as for the diagnostics of various diseases of the human cardiovascular system. The known processes for isotope separation are commercially unviable in the case of thallium. This has prompted intense research directed towards the development of optical techniques for the isotopic enrichment of thallium [1 – 3].

The classical photoionisation approach to isotope separation involves the use of a large set of laser radiations, including tunable single-frequency radiation. To simplify the isotopic enrichment process and reduce its cost, it is advantageous to excite thallium atoms by a laser that utilises vapour of the corresponding thallium isotope [4]. In photochemical isotope separation, which takes advantage of selective chemical reactions involving long-lived states (for example, the thallium $6p\,^2P^o_{3/2}$ metastable state), it is convenient to use 535-nm self-terminating laser (STL) radiation in order to diagnose level populations.

On the other hand, as early as 1971 Petrash [5] inferred from the energy level structure of thallium that lasing on the $7s\,^2S_{1/2} - 6p\,^2P^o_{3/2}$ transition would have high quantum efficiency ($\eta_q = 0.47$), the highest among metal vapour STLs $\{\eta_q = (h\nu/E_2)[g_1/(g_1 + g_2)]$, where $h\nu$ is the laser transition energy; E_2 is the energy of the upper laser level; and g_1 and g_2 are the statistical weights of the lower and upper levels, respectively$\}$. The properties of thallium lasers have been examined in a limited number of studies. Isaev et al. [6, 7] demonstrated superfluorescent emission at 535 nm in 'hard-pumped' (50 kV) small discharge tubes (0.13, 0.2, and 0.3 cm in diameter and 20 cm in length). A later study [8] addressed processes resulting in a population inversion and the behaviour of pulsed 535-nm superfluorescence during discharge excitation of thallium iodide vapour. In those studies, no energy characteristics were measured and, accordingly, neither the real lasing efficiency η_{real} ($\eta_{real} = P_{las}/P$, where P_{las} is the average lasing power and P is the pump power) nor the limiting efficiency η_{lim} ($\eta_{lim} = w_{las}/w$, where w_{las} is the lasing energy and w is the pump energy at the end of a laser pulse) were discussed.

This work examines the performance parameters of a gas-discharge thallium laser operating on the $7s\,^2S_{1/2} - 6p\,^2P^o_{3/2}$ transition ($\lambda = 535$ nm).

2. Experimental setup

Thallium lasers are typical metal vapour STLs. The upper laser level is the thallium $7s\,^2S_{1/2}$ resonance state (RS), and the lower level is the $6p\,^2P^o_{3/2}$ metastable state (MS) (Fig. 1). Population inversion is due to predominant excitation of thallium atoms to the $7s\,^2S_{1/2}$ state at the front of a current pulse. The high pulse repetition rate is due to the electron deexcitation of the $6p\,^2P^o_{3/2}$ state [9]. When an STL is pumped by a gas discharge, particular attention is paid to the inductances of the discharge tube and power supply, which must allow the formation of pump pulses with sharp edges. It seems likely that these requirements are more stringent for the thallium laser in comparison with, e.g., the copper vapour laser, because the RS lifetime of atomic thallium (governed by the probability of spontaneous

P.A. Bokhan, Dm.E. Zakrevskii, M.A. Lavrukhin Institute of Semiconductor Physics, Siberian Branch, Russian Academy of Sciences, prosp. Akad. Lavrent'eva 13, 630090 Novosibirsk, Russia; e-mail: bokhan@isp.nsc.ru, zakrdm@isp.nsc.ru

Received 12 March 2009
Kvantovaya Elektronika **39** (10) 911 – 916 (2009)
Translated by O.M. Tsarev

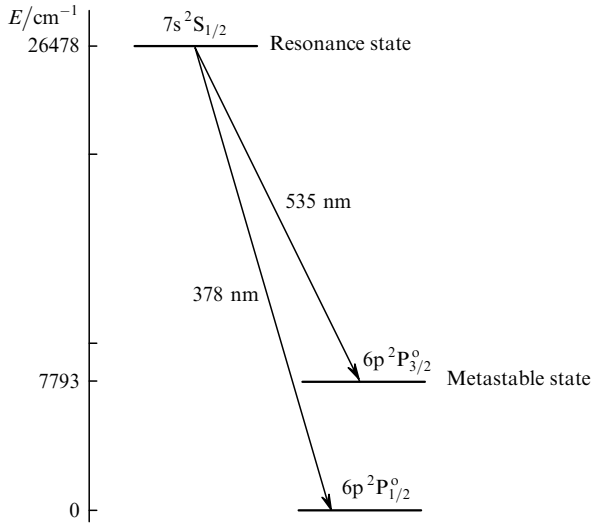

Figure 1. Energy level diagram and transitions of atomic thallium.

emission on the laser transition) is ~ 14 ns [10], which is much shorter than that of atomic copper (~ 1 μs).

The active element of the laser (Fig. 2) had the form of a beryllium oxide tube (*1*) with an inner diameter of 1.5 cm, length of 40 cm and wall thickness of 0.33 cm. The coaxial inner tantalum electrodes (*2*, *3*) formed a 40-cm-long discharge channel. The tube was surrounded by a coaxial current return lead (*4*) made from stainless steel foil. This configuration allowed the inductance of the tube to be reduced to ~ 30 nH. At 1000 °C, tubes of this geometry withstand a dc voltage of 20 kV applied between their inner and outer surfaces for a long time. The tube was enclosed in a vacuum-tight quartz casing (*5*) embedded in a resistance furnace (*6*). The tube was connected to a gas/vacuum system and operated either under sealed off vacuum conditions or at a low flow rate of an inert gas (helium or neon).

The power was supplied by discharging a capacitor on a load through a switch. The switches used were TGI1-1000/25 and TPI3-10k/25 thyratrons. The switch and the power bus lines were configured so as to minimise the parasitic inductances of the power supply circuit. As a result, the calculated total inductance of the power supply and discharge tube was ~ 70 nH. Peaking capacitors did not improve the lasing performance and so were not used.

The cavity was formed by an aluminium or dielectric mirror of 9-m radius of curvature and a flat quartz plate. In optical measurements, we used a coaxial vacuum photodiode with a resolution of ~ 300 ps. Electrical parameters were monitored with a Tektronix TDS2024B 200-MHz oscilloscope.

3. Experimental results

After thorough degassing at ~ 1000 °C, pieces of metallic thallium were evenly placed along the entire length of the discharge tube. In initial experiments, a thallium vapour/helium mixture was excited, using a TGI1-1000/25 thyratron as the switch. The tube generated pump pulses with the following parameters: voltage, up to 24 kV; full width at half maximum (FWHM), ~ 70 ns; leading edge width, ~ 30 ns. Over the entire range of excitation parameters examined, only spontaneous emission at 535 nm on the $7s\,^2S_{1/2} - 6p\,^2P^o_{3/2}$ transition was observed, with no coherent emission.

In subsequent experiments, a TPI3-10k/25 cold-cathode thyratron was used as the switch. It offers a number of advantages, including a considerably higher maximum rate of anode current rise (5×10^{11} A s^{-1} [11, 12] against the 4×10^9 A s^{-1} with the TGI1-1000/25). This thyratron has a tetrode configuration, which includes, in addition to a control electrode (grid), an auxiliary, preionisation electrode. This requires a double-pulse drive circuit. Figure 3a shows typical oscilloscope traces of the preionisation and trigger pulses in the TPI3-10k/25. As shown in our experiments, the rise time of the load voltage pulse is minimal at the minimal time delay (τ_{del}) between discharge initiation in the preionisation circuit ($t \approx 500$ ns in Fig. 3a) and triggering of the thyratron (the trigger pulse is at the trailing edge of the preionisation pulse). Triggering is then, however, unstable because of the jitter between the trigger and preionisation pulses. The optimal τ_{del} is $\sim 300 - 400$ ns. When a 680-pF capacitor is discharged on a 50-Ω resistive load in the frequency regime, at a leading edge width of the trigger pulse (Fig. 3a, pulse *2*) below 30 ns the leading edge width of the voltage pulse may be as small as $\sim 2.5 - 5$ ns (Fig. 3b). This makes the TPI3-10k/25 attractive as a switch for pumping lasers that are in an ionisation-induced non-equilibrium state.

Buffer gas/thallium vapour mixtures were excited using TPI3-10k/25 in a wide range of experimental conditions. Stable laser action at 535 nm on the $7s\,^2S_{1/2} - 7p\,^2P^o_{3/2}$ transition was achieved at buffer gas (neon or helium) pressures $p_{Ne(He)} = 2 - 5$ Torr, voltages across the rectifier $V_p = 8 - 24$ V, pump pulse repetition rates $f = 0.75-$

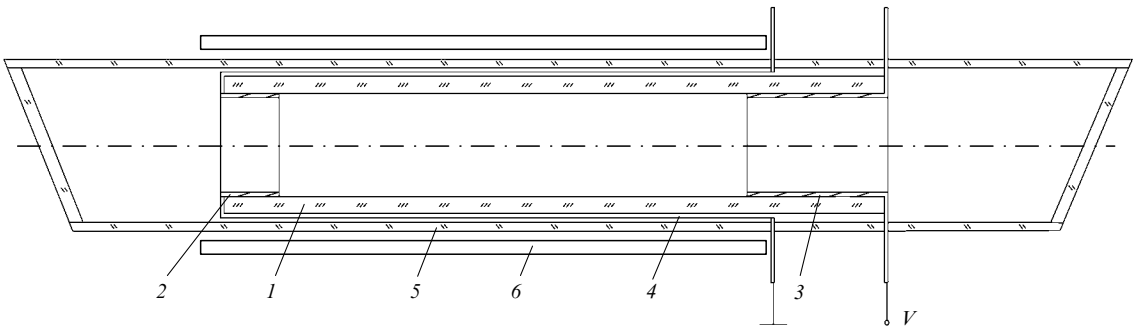

Figure 2. Discharge tube of the thallium laser: (*1*) beryllium oxide tube; (*2*) anode; (*3*) cathode; (*4*) current return lead; (*5*) quartz casing; (*6*) resistance heater.

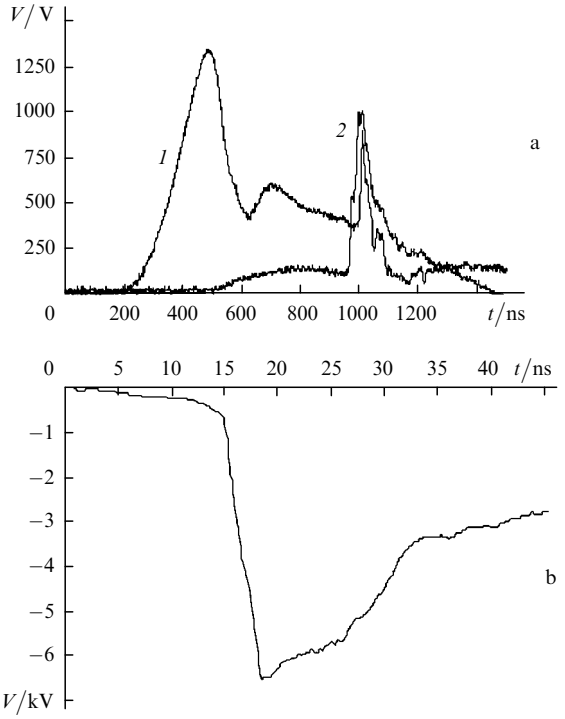

Figure 3. Oscilloscope traces of (a) the preionisation (*1*) and trigger (*2*) pulses in the TPI3-10k/25 thyratron and (b) a 50-Ω load voltage pulse ($C = 680$ pF).

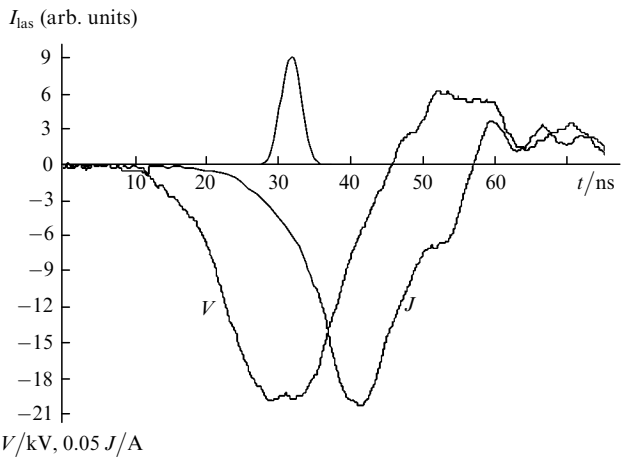

Figure 4. Oscilloscope traces of voltage (V), current (J) and lasing (I_{las}) pulses; $p_{Ne} = 2.2$ Torr, $p_{Tl} = 6 \times 10^{-2}$ Torr, $f = 1.45$ kHz.

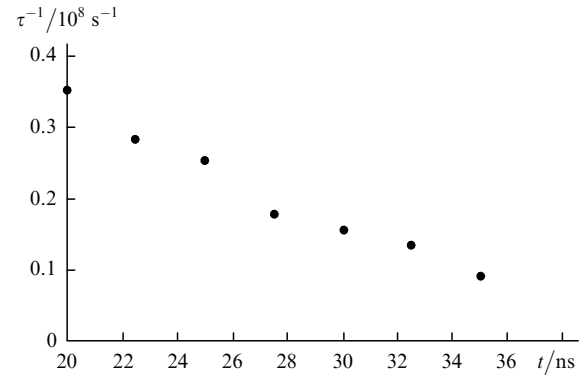

Figure 5. Time dependence of $1/\tau$, the parameter characterising the rise of the current through the discharge tube (same conditions as represented in Fig. 4).

5 kHz, working capacitances $C = 300 - 800$ pF and thallium vapour pressures $p_{Tl} \sim (0.8 - 9) \times 10^{-2}$ Torr.

The buffer gases used in our experiments were helium and neon, and the average lasing power, P_{las}, was found to be weakly dependent on the nature of the gas. At the same time, neon ensured more stable discharge initiation, so subsequent experiments were performed with this gas. The presence of a quartz plate as an output coupler had no effect on P_{las}, so our experiments were carried out in the superfluorescent regime, with the cavity formed by only one highly reflective mirror. The nature of the mirror had no effect on the superfluorescence parameters.

Figure 4 shows typical oscilloscope traces of discharge voltage (V), discharge current (J) and 535-nm lasing (I_{las}) pulses. At $p_{Ne} = 2.2$ Torr, $p_{Tl} = 6 \times 10^{-2}$ Torr, $f = 1.45$ kHz and $C = 470$ pF, the leading edge width of the voltage pulse was no greater than 15 ns. The longer pulse duration in comparison with a purely resistive load is due to the parasitic capacitances of the discharge tube and power supply circuit. The current rises more slowly than the voltage applied to the tube. The process can be represented by an exponential with variable $1/\tau$ (Fig. 5): $J = J_0 \exp[t/\tau(t)]$. During the lasing pulse, the rate of current rise reaches ~ 20 A ns^{-1} (Fig. 4), which is well below the maximum rate, determined by the inductance of the power supply circuit (~ 300 A ns^{-1}). Therefore, in this stage of the discharge, the tube can be considered an Ohmic load ($R \approx 150$ Ω at the maximum of the lasing pulse). In the final stage of the discharge, the resistance of the tube drops to ~ 12 Ω, and discharge oscillations develop. In the oscillatory regime, the current pulse width at the baseline level is $\tau_J = \pi\sqrt{L_p C} \approx 20$ ns (L_p is the parasitic inductance and C is the working capacitance). With a fully matched load, it was ~ 40 ns, whereas the experimentally determined value (not including the initial portion of the pulse before $t = 25$ ns) $\tau_J = 33$ ns. This points to high quality of load matching: the height of positive surges in oscilloscope traces of voltage and current pulses was 30 % and 20 % of the pulse height, respectively.

Under optimal excitation conditions, the lasing pulse was situated at the centre of the voltage pulse, at a current about one-third of the maximum level, and its FWHM was ~ 3 ns and depended only weakly on excitation conditions.

The average lasing power, P_{las}, increases with voltage across the rectifier (and, hence, with pump power), up to the maximum voltage of the thyratron (Fig. 6), and reaches ~ 7 mW, which gives a real lasing efficiency $\eta_{real} < 0.01$ %.

Figures 7 and 8 demonstrate the ranges of operating conditions for the gas-discharge thallium laser. The plots of the output power versus tube temperature (metal vapour pressure) (Fig. 7a) and neon buffer gas pressure (Fig. 7b) show a maximum and are typical of STLs. The optimal tube temperature in this study, ~ 670 °C, with $p_{Tl} \sim 6 \times 10^{-2}$ Torr, is lower than that reported by Petrash [5]: ~ 800 °C ($p_{Tl} \approx 1$ Torr).

The average output power and efficiency as functions of the pulse repetition rate are presented in Fig. 8. As seen in Fig. 8a, the optimal pump pulse repetition rate in the thallium laser ($p_{Ne} = 2.2$ Torr, $V_p = 18$ kV, $p_{Tl} = 6 \times 10^{-2}$ Torr) is no higher than 2 kHz. For $f > 2.5$ kHz, no lasing occurs.

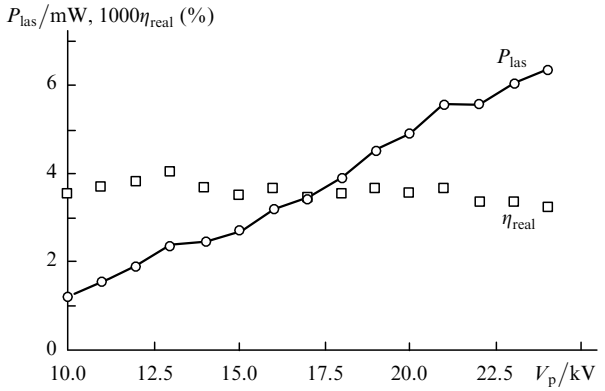

Figure 6. Average lasing power, P_{las}, and lasing efficiency, η_{real}, as functions of the voltage across the rectifier, V_p; $p_{Ne} = 2.2$ Torr, $p_{Tl} = 6 \times 10^{-2}$ Torr, $f = 1.45$ kHz, $C = 470$ pF.

Molecular additives to the gain medium of metal vapour STLs often have a beneficial effect on their power parameters [13–15]. In this study, bismuth vapour and hydrogen were added to neon-thallium active media using a separate source. Figure 8b illustrates the performance of the thallium laser ($C = 610$ pF, $p_{Ne} = 2.5$ Torr, $V_p = 18$ kV, $p_{Tl} = 6 \times 10^{-2}$ Torr) at hydrogen pressures of $\sim 2 \times 10^{-2}$, 3.2×10^{-2} and 8×10^{-2} Torr. Hydrogen additions are seen to influence the performance parameters of the laser; in particular, they raise the optimal frequency and reduce the lasing energy. The maximum average output power drops at any hydrogen pressure.

The addition of bismuth vapour to a neon-thallium mixture increased both the optimal (up to 3 kHz, Fig. 8b) and limiting pump pulse repetition rates. In the working temperature range of the thallium laser, bismuth vapour contains, in addition to atomic bismuth, $\sim 30\%$ Bi_2 dimers [16]. The total bismuth vapour pressure was $\sim 7 \times 10^{-1}$ Torr (accordingly, $p_{Tl} \sim 6 \times 10^{-2}$ Torr). The addition of bismuth vapour also increased the average output power and reduced the lasing energy and efficiency.

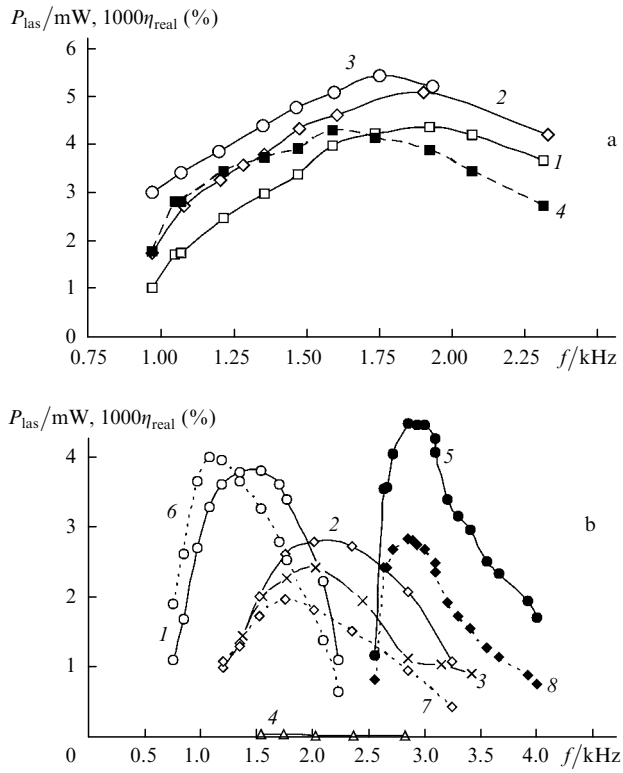

Figure 8. Average power and efficiency of the thallium laser as functions of pulse repetition rate. (a) P_{las} (*1–3*), η_{real} (*4*); Ne–Tl mixture; $C = 360$ (*1*, *4*), 610 (*2*) and 700 pF (*3*); $V_p = 18$ kV; $p_{Ne} = 2.2$ Torr; $p_{Tl} = 6 \times 10^{-2}$ Torr. (b) P_{las} (*1–3*), η_{real} (*6–8*); Ne–Tl (*1*, *6*), Ne–Tl–H_2 (*2–4*, *7*) and Ne–Tl–Bi(Bi_2) (*5*, *8*) mixtures; $p_{H_2} = 2 \times 10^{-2}$ (*2*, *7*), 3.2×10^{-2} (*3*) and 8×10^{-2} Torr (*4*) ($C = 610$ pF, $p_{Ne} = 2.5$ Torr, $V_p = 18$ kV, $p_{Tl} = 6 \times 10^{-2}$ Torr).

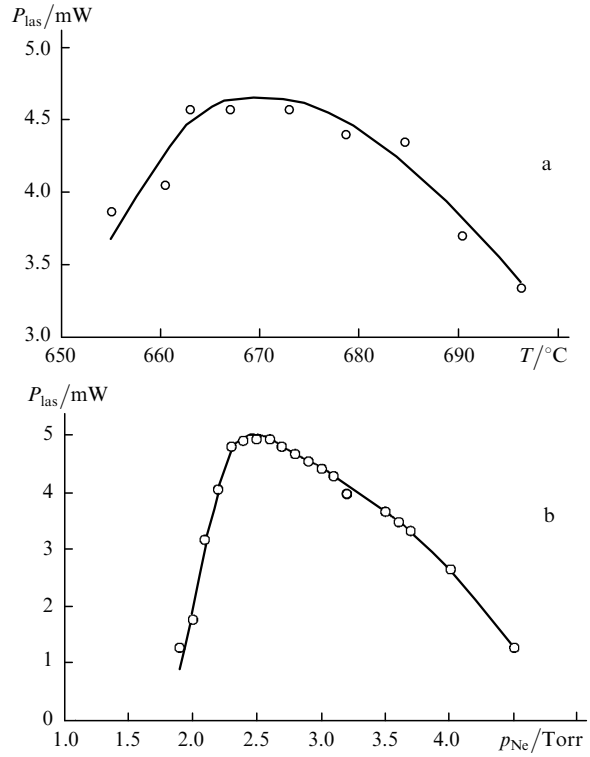

Figure 7. Average lasing power, P_{las}, as a function of (a) tube temperature ($V_p = 20$ kV, $p_{Ne} = 3$ Torr, $f = 1.45$ kHz) and (b) neon pressure ($V_p = 20$ kV, $p_{Tl} = 6 \times 10^{-2}$ Torr, $f = 1.45$ kHz).

4. Discussion

4.1 Power parameters

One distinctive feature of atomic thallium is the short lifetime (~ 14 ns) of its RS, determined by the probability of spontaneous emission on the laser transition [10]. The measured laser pulse duration is even shorter (~ 3 ns), and the actual pulse duration, corrected for the photodetector and oscilloscope passbands, is under 2 ns. Therefore, to achieve efficient lasing, a high population of the upper laser level must be created in a time comparable to the laser pulse duration at the baseline level (~ 5 ns). Consequently, to ensure efficient pump power conversion and, accordingly, acceptable output power, the current rise time of the pump pulse must be less than 5 ns. In this study, the rise time of the voltage applied to the discharge tube is ~ 12 ns, which is obviously too long for efficient power delivery to the active medium. Under the conditions of this study, even though the rate of current rise was faster than that typical of the copper vapour laser, the rate needed for the optimal

operation of the thallium laser was not reached. Since the rate of current rise in our experiments was substantially slower than the inductance-limited rate, it was obviously controlled by the rate of plasma generation in the tube. Therefore, the key to raising the lasing energy and efficiency lies in further increasing the voltage and reducing the working capacitance. This conclusion is supported by the fact that η_{real} is a weak function of V_p (Fig. 6), which corresponds to a quadratic dependence of P_{las} on V_p.

Let us estimate the limiting lasing efficiency, η_{lim}. It follows from the oscilloscope traces in Fig. 4 that the pump energy at the end of a laser pulse, w, is ~ 26 mJ, which corresponds to $\eta_{lim} \approx 0.013\,\%$. This is substantially lower compared to the copper vapour laser. In addition to natural causes of the reduction in η_{lim}, pertaining to the specific features of laser level excitation, it is worth examining the role of the high radiative probability of the laser transition and the associated losses due to spontaneous emission. The minimum RS population can be estimated from the relation $N_{RS} \sim N_{ph}/\eta_q \approx 2.8 \times 10^{11}$ cm^{-3} ($N_{ph} = P_{las}/(hvVf)$ [$N_{ph} = P_{las}/(hvVf)$, V is the tube volume, and $\eta_q = 0.47$ is the quantum efficiency of the lasing process]. Knowing N_{RS}, we can estimate the power of spontaneous emission on the laser transition at the end of a laser pulse: $P_{sp} \geqslant hvN_{RS}AfV\tau_{las} \approx 4.5$ mW at $f = 1.45$ kHz (A is the spontaneous emission probability and τ_{las} is the laser pulse duration). This value is comparable to the laser output power ($P_{las} \approx 5$ mW under the conditions represented in Fig. 4). The loss rate is further increased through spontaneous emission amplification in nonaxial rays. At an inverse population density of 2.8×10^{11} cm^{-3}, the Doppler-broadened gain χ at 535 nm is ~ 2.17 cm^{-1}, which gives $\chi d \approx 3.25$ over the tube diameter. Consequently, with allowance for amplification, the spontaneous loss rate exceeds the laser output power by at least one order of magnitude.

Thus, when population inversion is fully utilised in an oscillator–amplifier system free of losses due to amplified spontaneous emission, like, e.g., in a helium laser [17], the laser output power and efficiency must increase by at least one order of magnitude, to 70 mW and 0.1 %. Such parameters would be of practical interest. Therefore, the performance of the thallium vapour laser can be brought to a level suitable for practical use only in an oscillator–amplifier system at discharge voltages well above those used in this study. Also attractive may be the use of semiconductor switches utilising tunnelling-assisted impact ionisation fronts [18], which enable the generation of pulses with subnanosecond leading edges at voltages of tens of kilovolts and kilohertz repetition frequencies. One can then use travelling wave excitation, which will markedly reduce the losses due to spontaneous emission.

To enhance the performance of STLs, use is often made of peaking capacitors, but in our experiments no positive results were obtained. One possible reason for this is that the parasitic capacitance of the power supply circuit, C_p, was used for this purpose. It follows from the oscilloscope traces in Fig. 4 that $C_p \approx \tau_V^2/(\pi^2 L_p) \approx 70$ pF, where τ_V is the rise time of the voltage pulse. It seems likely that, for optimal pumping, lower C_p is needed.

4.2 Pulse repetition frequency

A key issue in designing a high-average-power laser is its ability to operate at high pulse repetition rates (f). The limited increase in the power parameters of metal vapour STLs with increasing f is associated with either the insufficiently fast relaxation rate of the MS population or the slow plasma recombination between pulses. In the former case, the prepulse MS population is so high that it influences the pulse energy at increased f and, accordingly, reduces the average output power. In the latter case, the considerable prepulse electron concentration initiates many processes that have an adverse effect on lasing conditions, in particular, an increase in the pump rate of the lower laser level relative to the upper level.

To achieve a high laser output power, the metastable lower laser level must relax rapidly. One effective approach to depopulation of the lower laser level in metal vapour STLs is electron deexcitation [19]. An important feature of the thallium vapour laser is that its metastable lower laser level $^2P^o_{3/2}$, a fine-structure component of the $6p\,^2P^o$ ground state, lies ~ 1 eV above the other component, $6p\,^2P^o_{1/2}$. The effectiveness of MS relaxation in this system was examined in a previous study [9]. From the dependence of the relative 535-nm output power on the optical pump pulse delay relative to the discharge pulse, the rate constant for electron deexcitation of the $6p\,^2P^o_{3/2}$ MS, k_e was determined to be no less than 1.5×10^{-8} cm^{-3}s^{-1}. Taking that $\sim 30\,\%$ of the energy deposited in the discharge goes into ionisation [20], we obtain that the electron concentration at the end of a discharge pulse is $N_e \sim 3 \times 10^{14}$ cm^{-3}. At $k_e = 1.5 \times 10^{-8}$ cm^{-3} s^{-1}, the deexcitation rate of the thallium $6p\,^2P^o_{3/2}$ state is then $k_e N_e = 4.5 \times 10^6$ cm^{-1}. Therefore, the rate of intermixing of MS and ground-state atoms is so high that the MS population in the discharge afterglow is only determined by the electron temperature. Since current oscillations in the discharge afterglow cease by a time $t \sim 100$ ns, it is reasonable to assume that, as in the case of an optimised copper vapour laser [21], the prepulse MS population has no significant effect on the pulse repetition rate, which is then only limited because of the insufficient heating rate of the electron gas due to the high prepulse electron concentration and the long rise time of the voltage pulse. This is indirectly supported by the fact that we failed to achieve self-terminating laser action when the rise time of the pump pulse was ~ 30 ns.

The addition of hydrogen to the active medium of metal vapour STLs accelerates recombination processes between pulses, eventually reducing the prepulse electron concentration and raising the breakdown voltage and the optimal pulse repetition rate. However, the presence of molecular species in the active medium lowers the electron temperature reached during a pump pulse. Our results indicate that even small hydrogen additions reduce the lasing energy and power. This implies that, when the plasma contains molecular additions, the reduction in electron temperature during a pump pulse has a strong effect on the power parameters of the laser. Accordingly, the influence of prepulse electron concentration in the thallium laser is stronger in comparison with the copper vapour laser.

The effect of bismuth vapour on the performance parameters of the thallium laser, found accidentally in studies of a bismuth laser on the setup used in this work, turned out to be unpredictable. At the present stage, we have no satisfactory explanation for this behaviour.

5. Conclusions

We studied the performance parameters of a gas-discharge thallium laser operating on the $7s\,^2S_{1/2} - 6p\,^2P^o_{3/2}$ self-terminating transition ($\lambda = 535$ nm). The highest average output power achieved is ~ 7 mW. Even small hydrogen additions raise the optimal pump pulse repetition rate but reduce the lasing energy and average output power. The addition of bismuth vapour increases the optimal pulse repetition rate (up to 3 kHz) and average output power. Under the experimental conditions of this study, the real lasing efficiency does not exceed 0.01 % because of the inefficient delivery of the pump power to the active medium. The lasing efficiency achieved is 0.016 %. The high probability of spontaneous emission on the laser transition results in high losses due to spontaneous emission. At the end of a laser pulse, its power exceeds the output power by at least a factor of 10, with allowance for the amplification in nonaxial beams. To fully utilise the population inversion in the thallium laser and to raise its output power and efficiency, it is advantageous to use an oscillator–amplifier system free of losses due to amplified spontaneous emission and pump sources with a nanosecond rise time and a pump pulse duration comparable to the laser pulse duration.

Acknowledgements. We are grateful to A.I. Moshkunov for his suggestions regarding fast switching using the TPI3-10k/25 thyratron.

References

1. Kwang-Hoon Ko, Do-Young Jeong, Hyunmin Park, Taek-Soo Kim, Gwon Lim, Yong-Ho Cha. *J. Korean Phys. Soc.*, **51**, 327 (2007).
2. Bokhan P.A., Zakrevskii Dm.E., Kim V.A., Fateev N.V. *Opt. Spektrosk.*, **104**, 771 (2008).
3. Kim C.J., Park H., Ko K.H., Lim G., Kim T.S., Rho S., Cha Y.H., Han J., Jeong D.Y. *Proc. 10th Int. Workshop on Separation Phenomena in Liquids and Gases Angra Dos Reis* (Brazil, 2008).
4. Bokhan P.A., Zakrevskii Dm.E., Kim V.A., Fateev N.V. RF Patents No. 2 314 863 (2008) and No. 2 317 847 (2008).
5. Petrash G.G. *Usp. Fiz. Nauk*, **105**, 644 (1971).
6. Isaev A.A., Ishchenko P.I., Petrash G.G. *Pis'ma Zh. Eksp. Teor. Fiz.*, **6**, 619 (1967).
7. Isaev A.A., Petrash G.G. *Pis'ma Zh. Eksp. Teor. Fiz.*, **7**, 204 (1967).
8. Isaev A.A., Kazaryan M.A., Petrash G.G. *Opt. Spektrosk.*, **31**, 332 (1971).
9. Bokhan P.A., Zakrevskii Dm.E., Kim V.A. *Kvantovaya Elektron.*, **38**, 1110 (2008) [*QuantumElectron.*, **38**, 1110 (2008)].
10. Gallagher A., Lurio A. *Phys. Rev.*, **136** (1A), A87 (1964).
11. www.pulsetech.com.
12. Anchugov O.V., Matveev Yu.G., Shvedov D.A., Bochkov V.D., Bochkov D.V., Dyagilev V.M., Ushich V.G., Mikhailov S.F., Popov V.G. *Proc. 15th IEEE Int. Pulsed Power Conf.* (Albuquerque, NM, USA, 2007) pp 1335–1338.
13. Bokhan P.A., Silant'ev V.I., Solomonov V.I. *Kvantovaya Elektron.*, **7**, 1264 (1980) [*Sov. J. Quantum Electron.*, **10**, 724 (1980)].
14. Astadjov D.N., Sabotinov N.V., Vuchkov N.K. *Opt. Commun.*, **56**, 279 (1985).
15. Bokhan P.A., Molodykh E.I., in *Pulsed Metal Vapour Lasers* (Dortrecht: Kluver Acad. Publ., 1996) Vol. 5, p. 137.
16. Nesmeyanov An.N. *Davlenie para khimicheskikh elementov* (Vapour Pressures of Chemical Elements) (Moscow: Akad. Nauk SSSR, 1961).
17. Bel'skaya E.V., Bokhan P.A., Zakrevskii Dm.E. *Kvantovaya Elektron.*, **38**, 823 (2008) [*Quantum Electron.*, **38**, 823 (2008)].
18. Lyubutin S.K., Rukin S.N., Slovikovsky B.G., Tsyranov S.N. *Pis'ma Zh. Tekh. Fiz.*, **31** (5), 36 (2005).
19. Bokhan P.A., *Kvantovaya Elektron.*, **13**, 1837 (1986) [*Sov. J. Quantum Electron.*, **16**, 1207 (1986)].
20. Borovich B.L., Yurchenko N.I. *Kvantovaya Elektron.*, **11**, 2081 (1984) [*Sov. J. Quantum Electron.*, **14**, 1391 (1984)].
21. Bokhan P.A., Zakrevskii Dm.E. *Kvantovaya Elektron.*, **32**, 602 (2002) [*Quantum Electron.*, **32**, 602 (2002)].